ELSEVIER

Micellar electrokinetic chromatography of long chain saturated and unsaturated free fatty acids with neutral micelles
Considerations regarding selectivity and resolution optimization

J. Collet, P. Gareil*

*Laboratoire d'Electrochimie et de Chimie Analytique (URA CNRS 216), Ecole Nationale Supérieure de Chimie de Paris,
11 Rue Pierre et Marie Curie, 75231 Paris Cedex 05, France*

Abstract

The separation of saturated and unsaturated long chain (C_{14}–C_{20}) free fatty acids (FFAs) was investigated by micellar electrokinetic chromatography (MEKC) in the presence of polyoxyethylene-23-dodecylether (Brij 35) micelles and methanol containing electrolytes and under the conditions of a cathodic electroosmotic flow (EOF). The detection was performed by indirect absorbance detection using *p*-methoxybenzoate (*p*-anisate) as absorbing co-ion in the electrolyte. This type of separation, featuring anionic analytes and neutral micelles, can be conveniently modelled by adapting the physico-chemical framework initially developed by Terabe et al. [Anal. Chem. 57 (1985) 834] for the case of neutral analytes and anionic micelles. It has been established that optimal resolution is obtained when the anionic analytes spend more time in the bulk hydroorganic electrolyte than in the neutral micellar pseudo-phase. This approach was implemented for optimizing the Brij 35 concentration and the methanol content in the electrolyte. It has also allowed us to determine chromatographic-type selectivity, which is a major issue for the assessment of alternate separation methods. Accordingly, the selectivity of Brij 35 micelles for the C_{16}–C_{18} FFA pair was quite similar to that currently obtained in gas chromatography. Finally, this work demonstrates that MEKC is a cost and time effective method for the separation of critical pairs of saturated and unsaturated FFAs of identical equivalent chain length.   © 1997 Elsevier Science B.V.

Keywords: Selectivity; Resolution; Buffer composition; Fatty acids

1. Introduction

The separation of free fatty acids (FFAs) is presently a real challenge for capillary electrophoresis (CE). Classically, the CE separation of a series of ionic surfactant homologues is based solely on the difference in their respective molecular masses, since they all bear the same electrical charge [1–7]. For surfactants having an alkyl chain length of less than 8–10 carbon atoms, this mass discrepancy is generally enough to achieve the baseline resolution of

surfactants differing by a single carbon atom in their alkyl chain. However, as the length of this chain increases, the relative difference in chain length between two consecutive homologues rapidly declines, and their separation becomes more difficult. Concomitantly, the solubility of such heavier surfactants in purely aqueous electrolytes eventually becomes a limiting factor, which cannot be satisfactorily circumvented by resorting to organic solvents only, since the analysis time would increase dramatically. Roldan-Assad and Gareil [8] showed that in the case of FFAs, the addition of neutral cyclodextrins to the separating electrolyte constitutes a

*Corresponding author.

valuable alternative to the use of hydroorganic media, as it allows one to fully resolve a linear saturated C_2–C_{14} FFA mixture. This approach also succeeded in separating a similar C_7–C_{18} mixture while keeping the methanol content in the electrolyte to a minimum. Collet and Gareil [9] later optimized the nature of the cyclodextrin to achieve the separation of saturated and unsaturated FFAs ranging between C_{14} and C_{18}. The presence of a cyclodextrin allows one to tune the separation selectivity, as far as the alkyl chain length, the number and position of carbon–carbon double bonds all strongly affect the formation constants of the involved inclusion complexes. Nevertheless, it appeared that the solubility enhancement produced by the cyclodextrins is limited to FFAs with a chain length inferior to ca. 18 carbon atoms, which can be understood, if one considers that the length of such a limiting FFA in a stretched configuration is of the order of 3 nm, and the depth of the hydrophobic cavity of a cyclodextrin is close to 0.8 nm. From this point of view, the heaviest FFAs are better solubilized by micellar systems than by cyclodextrins. Also, for the separation of a saturated C_8–C_{20} FFA mixture, Erim et al. [10] adopted a mixed micellar system comprised of a neutral surfactant with a polyoxyethylene polar head, Brij 35 and an anionic surfactant, sodium dodecyl benzenesulfonate, in an hydroorganic medium containing 50% acetonitrile. Brij 35 was selected for its high level of purity, high UV transparency and its very low critical micellar concentration (ca 0.1 mM). This latter criterion is of paramount importance as it generally testifies to the formation of micelles or related aggregates in the studied hydroorganic media. Apart from the separation of standard saturated FFA mixtures, Erim et al. [10] also realized the quantitative analyses of samples of saponified butters and vegetal edible fats. Their method, however, was not optimized for the resolution of unsaturated FFAs, which led to a number of peak overlaps between saturated and unsaturated FFAs.

    The aim of this work was to enhance appreciation of the respective influences of the organic solvent content (methanol) and surfactant concentration (Brij 35) in the electrolyte on the solubility and the separation selectivity of saturated and unsaturated FFAs, in order to optimize the simultaneous sepa-

ration of compounds belonging to either of both classes. Such a result can be reached from a purely experimental approach, but also more theoretically through the use of a physicochemical model describing the behaviour of each analyte. The former approach was simply supported by a qualitative description of the chemical distribution equilibria involved, whereas the latter one, which is basically more quantitative and predictive, took advantage of the treatment initially developed by Terabe and coworkers [11,12] that yielded the resolution equation representing neutral analytes in the presence of anionic micelles. This treatment has been adapted to account for anionic analytes in the presence of neutral micelles.

2. Theoretical

2.1. Separation of neutral analytes in the presence of anionic micelles

    The treatment described here is that of micellar electrokinetic chromatography (MEKC) in its usual form, i.e., as it was first introduced by Terabe et al. [11] in 1984. It applies to the separation of neutral analytes in the presence of anionic micelles. Fig. 1 gives a scheme of an electropherogram depicting this situation. This section is just intended to re-establish the equations giving the retention factors and the
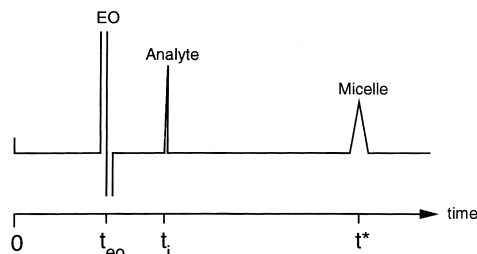

Fig. 1. Schematic drawing of an electropherogram in classical MEKC. Retention of a neutral solute (i) in the presence of anionic micelles and under the conditions of a strong cathodic EOF. The magnitude of this flow is assumed to be superior to that of the electrophoretic velocity of the micelles toward the anode. Sample injection on the anodic side, detection on the cathodic side. t_{eo}, t_i and t^* are the retention times of an EOF marker, of the solute i and of a micelle marker, respectively.

resolution and to place them in their context before contemplating a new case.

In analogy to conventional chromatography, the retention factor k' of an analyte i is defined in MEKC as the ratio of the analyte mole number solubilized by the micellar phase (n_i^*), to its mole number remaining in the aqueous phase (n_i^{aq}):

$$k_i' = \frac{n_i^*}{n_i^{aq}} = \frac{C_i^*}{C_i^{aq}} \cdot \frac{V^*}{V^{aq}} = K_i \cdot \frac{\bar{v}(C_t - CMC)}{1 - \bar{v}(C_t - CMC)} \quad (1)$$

where C_i^* and C_i^{aq} are the analyte concentrations in the micellar and aqueous phases, respectively, V^* and V^{aq}, the volume fractions occupied by both phases, K_i is the distribution coefficient of the analyte i; $\bar{v}$ is the surfactant partial molar volume, C_t is the total surfactant concentration in the electrolyte and CMC denotes the critical micellar concentration. If the surfactant concentration is not too high (<0.2 M), the term $\bar{v}(C_t - CMC)$ can be safely neglected with respect to 1, so that Eq. (1) reduces to:

$$k_i' \approx K_i \bar{v}(C_t - CMC) \quad (2)$$

Under this assumption the plot of k' versus C_t yields a straight line, the slope of which is proportional to K_i and the x-intercept provides the CMC value. The experimental access to the retention factor k' results from the relationship between the analyte, micelle and electroosmotic flow (EOF) velocities. In effect, the apparent analyte transport velocity along the capillary, ν_i, can be expressed as a weighted average of the electroosmotic velocity, ν_{eo}, and of the apparent velocity of the micelles, ν^*, both of which being affected by a coefficient representing the analyte molar fraction in each of the two phases:

$$\nu_i = \frac{n_i^{aq}}{n_i^{aq} + n_i^*} \cdot \nu_{eo} + \frac{n_i^*}{n_i^{aq} + n_i^*} \cdot \nu^*$$
$$= \frac{1}{1 + k_i'} \cdot \nu_{eo} + \frac{k_i'}{1 + k_i'} \cdot \nu^* \quad (3)$$

One can then derive the expression of the retention factor k_i' as a function of the retention time of the analyte, t_i, of an unretained neutral marker, t_{eo}, and of a micelle marker, t^*:

$$k_i' = \frac{\nu_{eo} - \nu_i}{\nu_i - \nu^*} = \frac{l/t_{eo} - l/t_i}{l/t_i - l/t^*} = \frac{t_i - t_{eo}}{t_{eo}(1 - t_i/t^*)} \quad (4)$$

t_i, t_{eo} and t^* are defined in Fig. 1. l is the capillary length from the injection end to the detector window. The reciprocal expression is:

$$t_i = \frac{(1 + k_i') \cdot t_{eo}}{1 + (t_{eo}/t^*) \cdot k_i'} \quad (5)$$

When t^* increases to infinity, Eq. (4) reduces to the classical form:

$$k_i' = \frac{t_i - t_{eo}}{t_{eo}} \quad (6)$$

Alternatively, the retention factors can also be profitably calculated by using mobilities as intermediate parameters. The concept of the pseudo-effective mobility of a neutral analyte in the presence of anionic micelles then needs to be introduced [13]:

$$m_i^{eff} = \frac{k_i'}{1 + k_i'} \cdot m_{eff}^* \quad (7)$$

which leads to:

$$k_i' = \frac{m_i^{eff}}{m_{eff}^* - m_i^{eff}} \quad (8)$$

Finally, the resolution of a pair of analytes 1 and 2 can be defined in MEKC keeping the general expression used in conventional chromatography:

$$R_s = 2 \cdot \frac{t_2 - t_1}{w_1 + w_2} \quad (9)$$

where w_i denotes the baseline peak width, expressed in time units, which can be related to the theoretical plate height through the expression:

$$N_i = 16 \left(\frac{t_i}{w_i} \right)^2 \quad (10)$$

w_1 and w_2 can often be considered equal if peaks 1 and 2 are very close to each other. Introducing the pseudo-effective mobilities, Eqs. (9) and (10) can be rearranged under the form:

$$R_s = \frac{1}{4} \cdot \left| \frac{m_1^{eff} - m_2^{eff}}{\bar{m}^{eff} + m_{eo}} \right| \sqrt{\bar{N}} \quad (11)$$

where $\bar{m}^{eff}$ and $\bar{N}$ denote the average pseudo-effective mobility and plate number, respectively, and m_{eo} the electroosmotic mobility. This equation holds for algebraic pseudo-effective mobilities. Besides, substituting Eqs. (5) and (10) into Eq. (9) leads to:

$$R_s = \frac{1}{4}\left(\frac{\alpha - 1}{\alpha}\right)\left(\frac{k_2'}{1 + k_2'}\right)\left(\frac{1 - t_{eo}/t^*}{1 + (t_{eo}/t^*)k_1'}\right)\sqrt{N_2} \quad (12)$$

in which α represents the separation selectivity, as usually defined:

$$\alpha = k_2'/k_1' = K_2/K_1 \quad (13)$$

analyte 2 being the later eluting compound, i.e., the compound having the strongest affinity for the micellar pseudo-phase. It can be noted that when t^* increses to infinity, Eq. (12) becomes equivalent to the Purnell relation in conventional chromatography. Importantly, the presence of the third bracketed term in Eq. (12) leads to an optimization strategy quite different from that followed in the presence of a real stationary phase. In the situation where the selectivity is low, $k_2' \approx k_1'$ and the following function of k', which was referred to by Foley [14] as the "retention term" should be maximized:

$$f(k') = \left(\frac{k'}{1 + k'}\right)\left(\frac{1 - t_{eo}/t^*}{1 + (t_{eo}/t^*)k'}\right) \quad (14)$$

The curves representing $f(k')$ versus k' for a constant value of the t_{eo}/t^* ratio (Fig. 2), go through a maximum for $k' = k_{opt}' \cdot k_{opt}'$ and $f(k_{opt}')$ are only dependent on the t_{eo}/t^* ratio:
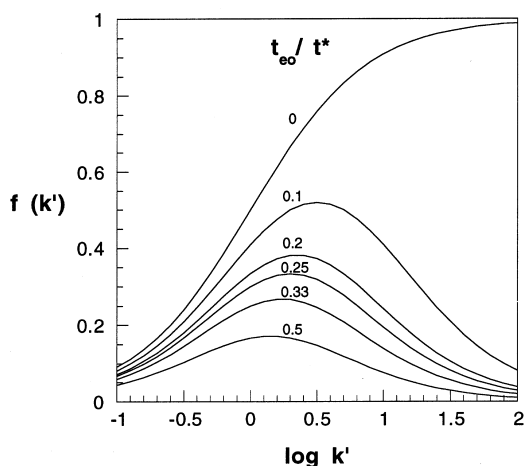
Fig. 2. Theoretical variations of the retention term $f(k')$ as a function of the retention factor k' for different values of the t_{eo}/t^* ratio. Calculations according to Eq. (14). See also Ref. [12].

$$k_{opt}' = \sqrt{t^*/t_{eo}} \quad (15)$$

$$f(k_{opt}') = \frac{1 - t_{eo}/t^*}{\left(1 + \sqrt{t_{eo}/t^*}\right)^2} \quad (16)$$

This ratio characterizes the span of the retention range accessible in MEKC. In common practice, it can be varied between 0.1 and 0.5, which gives corresponding k_{opt}' values in the range of from 1.4 to 3.2. k_{opt}' can also be expressed as a function of the electroosmotic mobility and the effective mobility of the micelles:

$$k_{opt}' = \left(\frac{m_{eo}}{m_{eo} + m_{eff}^*}\right)^{1/2} \quad (17)$$

The preceding relationships will remain entirely valid in the case of separation of neutral compounds in the presence of cationic micelles which would reverse the direction of the EOF and drag the cationic micelles to the anode, counter to their electrophoretic migration direction.

2.2. Separation of anionic analytes in the presence of neutral micelles: a new case

The principle of the separation of fatty acids by MEKC in the presence of neutral micelles of Brij 35 is illustrated in Figs. 3 and 4. The analytes can be separated according to a mixed mechanism of differential electromigration and differential partitioning between the aqueous and the micellar phase. Under alkaline conditions, the FFAs are all equally charged and their separation can only result from differences between their frictional coefficients and/or differences between their distribution coefficients K. It must be emphasized that, as the length of the alkyl chain of the acid increases, both mechanisms tend to move at a velocity closer to that of the EOF. This synergistic effect will help improve the separation of compounds that would not otherwise present sufficiently different friction coefficients. The separation of anionic solutes in the presence of neutral micelles appears to be a symmetrical situation with respect to what has just previously recalled in Section 2.1. Time can thus be spared in attempting to re-use the foregoing model and its associated optimization guidelines by adapting it through a mere change of variables: ν^* and t^* in the initial model must be
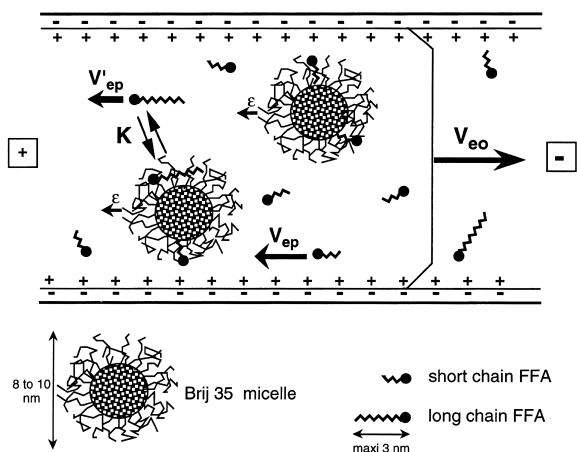
Fig. 3. Schematic of the separation principle of FFAs by MEKC in the presence of neutral Brij 35 micelles. Uncoated silica capillary, strong cathodic EOF. Sample injection on the anodic side, detection on the cathodic side. Depicted are the EOF velocity (ν_{eo}), the electrophoretic velocities of short- (ν_{ep}) and long- (ν'_{ep}) chain FFAs, the velocity (ε) of a solute incorporated to a micelle ($|\nu_{eo}| > |\nu_{ep}| > |\nu'_{ep}| > |\varepsilon|$), the distribution equilibrium of a solute (constant K) between the hydroorganic phase and the micellar pseudo-phase. The micellar solubilization can occur in the palisade region, formed by the polyoxyethylene chains of Brij 35, or in the micellar core, composed of C_{12} alkyl chains.

replaced by ν_{eo} and t_{eo}, respectively, while in turn ν_{eo} and t_{eo} must be respectively replaced by the velocity ν_z and migration time t_z of the charge analyte in the absence of the neutral micelles (i.e., in zone electrophoresis). Starting from Eq. (4), the retention factor $\tilde{k}'$ for this case is then expressed as:
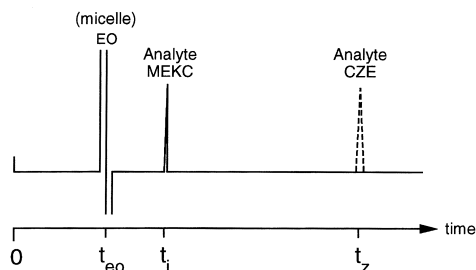

Fig. 4. Schematic drawing of an electropherogram obtained under the conditions of Fig. 3 (full line). Retention of an anionic solute in the presence of neutral micelles and under the conditions of a strong cathodic EOF. Sample injection on the anodic side, detection on the cathodic side. t_{eo}, retention time of both an EOF marker and of a micelle marker. t_i, retention time of solute i. The peak corresponding to the migration of the solute in the absence of micelles (migration time, t_z) is represented by a dashed line.

$$\tilde{k}' = \frac{t_i - t_z}{t_z(1 - t_i/t_{eo})} \tag{18}$$

This last relationship calls for two comments. First, it would be preferable to call $\tilde{k}'$ "affinity factor" rather than "retention factor" in this case. The former name does not make a connection with the order of detection of the analytes, and so is not ambiguous here. Secondly, it is worth noting that t_z in Eq. (18) is not directly accessible to experiment and can only be calculated. In effect, the electroosmotic mobility can be strongly dependent on the surfactant concentration in the electrolyte, so that the analyte migration time that can be experimentally measured in the absence of micelles (denoted t_i^z) must be distinguished from what would be obtained under the electroosmotic conditions of the MEKC experiment (denoted t_i^0). Eventually, the practical calculation of $\tilde{k}'$ should be performed in two steps, according to equations:

$$\tilde{k}'_i = \frac{t_i^m - t_i^0}{t_i^0(1 - t_i^m/t_{eo}^m)} \tag{19}$$

$$t_i^0 = \frac{L \cdot l}{V} \cdot \frac{1}{(m_{eo}^m + m_{eff_i}^z)} \tag{20}$$

where i is the analyte index and the superscripts ^{m} and ^{z} stand for the presence or the absence of micelles, respectively. For the sake of simplicity, calculations of the affinity factors will be better conducted using the effective mobilities, which are independent of the electroosmotic conditions. The analogue of Eq. (7) can be written as:

$$m_{eff_i}^m = \frac{1}{1 + \tilde{k}'_i} \cdot m_{eff_i}^z \tag{21}$$

which yields:

$$\tilde{k}'_i = \frac{m_{eff_i}^z}{m_{eff_i}^m} - 1 \tag{22}$$

$m_{eff_i}^z$ and $m_{eff_i}^m$ represent the effective mobilities of analyte i that can be determined experimentally in the absence, or in the presence of the neutral surfactant, respectively:

$$m_{\mathrm{eff}_i}^{\mathrm{z}} = m_{\mathrm{app}_i}^{\mathrm{z}} - m_{\mathrm{eo}}^{\mathrm{z}} = \frac{L \cdot l}{V}\left(\frac{1}{t_i^{\mathrm{z}}} - \frac{1}{t_{\mathrm{eo}}^{\mathrm{z}}}\right) \tag{23}$$

$$m_{\mathrm{eff}_i}^{\mathrm{m}} = m_{\mathrm{app}_i}^{\mathrm{m}} - m_{\mathrm{eo}}^{\mathrm{m}} = \frac{L \cdot l}{V}\left(\frac{1}{t_i^{\mathrm{m}}} - \frac{1}{t_{\mathrm{eo}}^{\mathrm{m}}}\right) \tag{24}$$

The classical resolution equation developed by Terabe (Eq. (12)) can also be applied to this new case under the additional assumption that the two solutes of the pair have identical effective mobilities in the absence of the micelles [15,16]. In such a case, $t_1^0 = t_2^0 = t^0$ and:

$$R_s = \frac{1}{4}(\alpha - 1)\left(\frac{\tilde{k}_2'}{1 + \tilde{k}_2'}\right)\left(\frac{t^0/t_{\mathrm{eo}} - 1}{1 + (t^0/t_{\mathrm{eo}})\tilde{k}_1'}\right)\sqrt{N_2} \tag{25}$$

with

$$\alpha = \tilde{k}_1'/\tilde{k}_2' = K_1/K_2 \tag{26}$$

and, for the so-called retention term:

$$\mathrm{f}(\tilde{k}') = \left(\frac{\tilde{k}'}{1 + \tilde{k}'}\right)\left(\frac{t^0/t_{\mathrm{eo}} - 1}{1 + (t^0/t_{\mathrm{eo}})\tilde{k}'}\right) \tag{27}$$

Note that now $t_2^{\mathrm{m}} > t_1^{\mathrm{m}}$ implies $\tilde{k}_1' > \tilde{k}_2'$.

Fig. 5 shows the theoretical variation of the retention term $\mathrm{f}(\tilde{k}')$ as a function of $\tilde{k}'$. It must be recognized that the functions $\mathrm{f}(k')$ (Eq. (14)) and
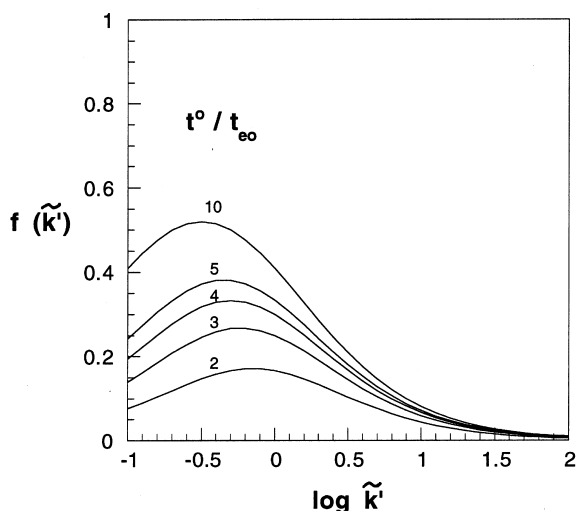

Fig. 5. Theoretical variations of the retention term $\mathrm{f}(\tilde{k}')$ as a function of the affinity factor $\tilde{k}'$ for different values of the t_{eo}/t^* ratio. Calculations according to Eq. (27).
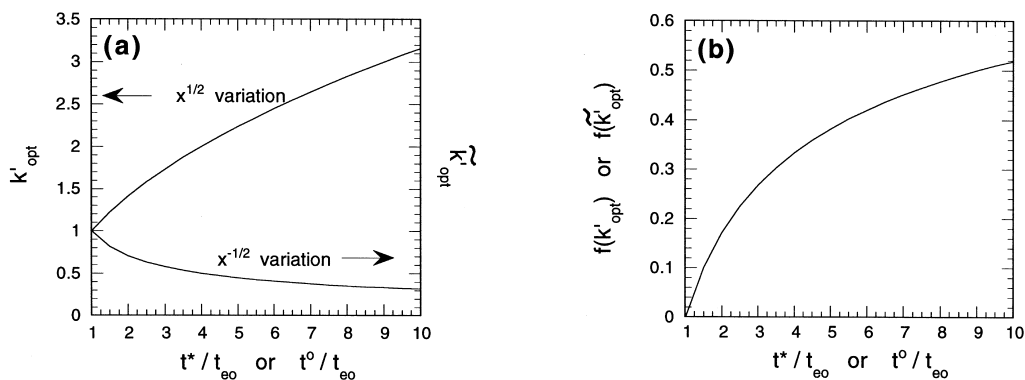
$\mathrm{f}(\tilde{k}')$ (Eq. (27)) can be put in the common consistent form:

$$|\mathrm{f}_x(k')| = \left|\left(\frac{k'}{1 + \tilde{k}'}\right)\left(\frac{1 - x}{1 + xk'}\right)\right| \tag{28}$$

with $x = t_{\mathrm{eo}}/t^*$ for Eq. (14) or $x = t^0/t_{\mathrm{eo}}$ for Eq. (27). This function goes through a maximum for:

$$k_{\mathrm{opt}}' = \sqrt{1/x} \tag{29}$$

which is

$$\mathrm{f}_x(k_{\mathrm{opt}}') = \frac{1 - x}{(1 + \sqrt{x})^2} \tag{30}$$

Fig. 6a represents the variation of the optimal retention factor k_{opt}' and the optimal affinity factor $\tilde{k}_{\mathrm{opt}}'$, as a function of t^*/t_{eo} and t^0/t_{eo} ratios, respectively. This is the first interesting result of this approach, insofar as it dictates the choice of the optimal surfactant concentration. It appears that k_{opt}' is always greater than unity while $\tilde{k}_{\mathrm{opt}}'$ is always inferior. In other words, the achievement of the highest resolution requires that the neutral analytes should spend more time in the ionic micellar pseudophase than in the aqueous phase while the reverse is true when use is made of neutral micelles to separate anionic solutes. Another interesting point can be derived from the following remarkable property:

$$\forall x, \mathrm{f}_{1/x}(k_{\mathrm{opt}}') = -\mathrm{f}_x(k_{\mathrm{opt}}') \tag{31}$$

As illustrated in Fig. 6b, the resolution performances of ionic micelles with respect to neutral analytes and of neutral micelles with respect to anionic analytes of equal effective mobilities will be identical if the retention ranges are the same ($t^*/t_{\mathrm{eo}} = t^0/t_{\mathrm{eo}}$).

3. Experimental

3.1. Instrumentation

The measurements were carried out with a Waters Quanta 4000 capillary electrophoresis system (Waters, Milford, MA, USA) equipped with a 35 cm long (27.5 cm to the detector cell)×50 μm I.D. fused-silica capillary column, obtained from Supelco (Bellefonte, PA, USA). All experiments were per-

Fig. 6. Dependence of (a) the optimal retention factor (k'_{opt}) and optimal affinity factor ($\tilde{k}'_{opt}$) and (b) f(k'_{opt}) and f($\tilde{k}'_{opt}$) on t^*/t_{eo} and t^0/t_{eo} ratios, respectively. Calculations from Eqs. (29) and (30).

formed at room temperature (approx. 25°C) and constant voltage ($V = +30$ kV), under normal polarity (anode at the inlet). Samples were introduced by creating a 10 cm difference between the levels of the inlet vial and the outlet reservoir for 5 s (gravity mode). Solutes were monitored by indirect UV absorbance detection at 254 nm, using the mercury vapor lamp of the instrument. Detector signals were collected with a NEC Powermate 386/25 computer and processed with the Waters Maxima software.

3.2. Chemicals

Fatty acids, Brij 35 (polyoxyethylene-23-lauryl ether) and other background electrolyte components were obtained from Aldrich (Milwaukee, WI, USA) or Sigma (St. Louis, MO, USA). Tris–anisate electrolytes were prepared by partially neutralizing Tris base with *p*-anisic (*p*-methoxybenzoic) acid (both from Aldrich) to pH 8.1 (pH measured before the addition of methanol).

3.3. Procedure

Purified water from an Alpha-Q system (Millipore, Bedord, MA, USA) was used to prepare buffers and standard solutions. All carrier electrolytes were filtered through 0.45 μm Millex-HV filter units (Millipore) and degassed for 10 min in an ultrasonic bath before use. The capillary was systematically rinsed with the electrolyte (2 min) between runs, corresponding to the displacement of six capillary

volumes. Fatty acid stock sample solutions were prepared in methanol at a concentration of 1 g/l and stored at 4°C to prevent chemical decomposition and isomerisation of polyunsaturated fatty acids (PUFAs). These stock solutions were then diluted in the electrolyte to obtain a mixture containing approximately $2 \cdot 10^{-4}$ *M* of each acid.

4. Results and discussion

4.1. Optimization of a mixture of saturated and unsaturated FFAs by MEKC

In this study, the impact of the two main parameters, methanol content and Brij 35 concentration in the electrolyte, was investigated in depth. These parameters govern the resolution, the analysis time as well as the signal-to-noise ratio for the indirect absorbance conditions that were employed. The range of solvent content to be studied was limited on its lower side because the resolution is impaired due to excessively high affinity factors and on its upper side because the analyte solubility gets poor as a result of the increase in Brij 35 CMC and the subsequent decrease in micelle concentration. The range of Brij 35 concentration is likewise limited by a resolution constraint on its upper side and by a solubility constraint on its lower side.

Fig. 7 shows the influence of the Brij 35 concentration added to the electrolyte on the FFA effective mobilities for three different contents in
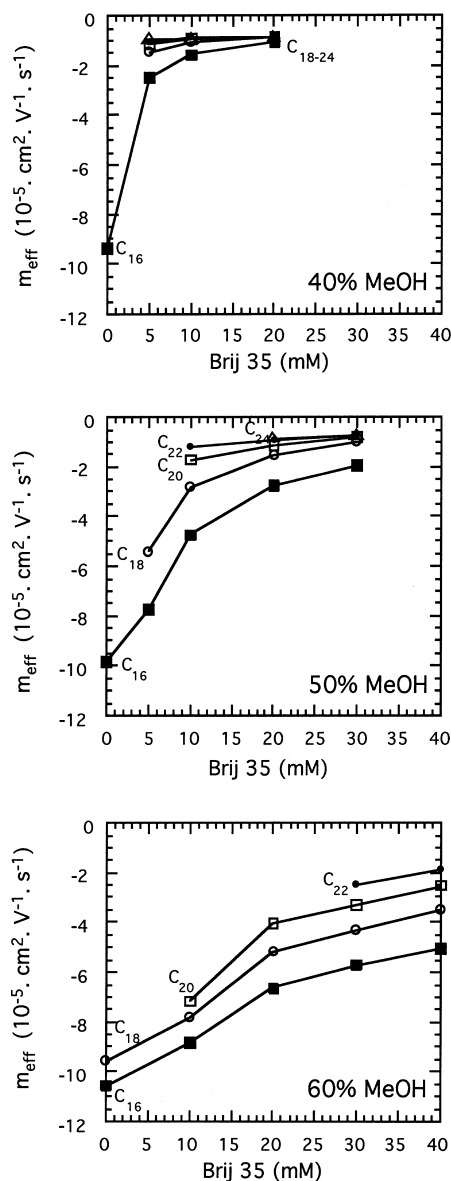
Fig. 7. Experimental variations of FFA (C_{16}–C_{24}) effective mobilities as a function of Brij 35 concentration for various methanol contents in the electrolyte. Fused-silica capillary, 35 cm (27.5 cm to the detector cell)×50 μm I.D. Electrolyte, 10 m*M* Tris–5 m*M* *p*-anisate (pH 8.1, measured before the addition of methanol). Applied voltage, 30 kV. Temperature, 25°C. Indirect absorbance detection at 254 nm. Gravity injection for 5 s (injection volume, 2 nl).

methanol (40, 50 and 60%, v/v). This series of experiments was conducted with linear saturated FFAs ranging between C_{16} and C_{24}. The FFAs having longer alkyl chains than C_{24} occur more scarcely in natural products and their solubilization becomes very spiny. On the other hand, the study of FFAs shorter than the C_{16} one was of less interest because these acids can be fully solubilized without Brij 35 micelles, simply using hydroorganic mixtures containing 40% methanol or higher. Toward this end, the total solubilization of a given FFA in an electrolyte was assessed by comparing the corrected surface area of this acid to that of the C_{16} FFA, present at the same concentration (ca. $2 \cdot 10^{-4}$ *M*) in the sample mixture as a standard. In Fig. 7, the mobility data of FFAs, for which a given electrolyte composition provided incomplete solubilization, were not reported. This was the case, especially, for the lowest levels of Brij 35 and methanol contents. With 40% methanol in the electrolyte, the micellar solubilization of the studied FFAs was abruptly obtained as soon as the CMC is exceeded (<5 m*M*). Without Brij 35 micelles, only the C_{16} FFA was soluble, whereas the presence of 5 m*M* Brij 35 succeeded in solubilizing the FFAs up to a C_{24} chain, but their resolution was not achieved. A hit-or-miss behaviour was thus observed. In contrast, with 60% methanol, the impact of the Brij 35 concentration on the effective mobilities was much more progressive at the expense of the C_{22} and C_{24} FFAs solubilization. This behaviour was likely to result from the enhancement of Brij 35 CMC. It may also reflect a more subtle change in the micelle characteristics (aggregation number, polydispersity or shape). Finally, the results obtained with the electrolyte containing 50% methanol constitute the best compromise with respect to sample solubility and resolution.

Fig. 8 represents the quasi-linear decrease of the electroosmotic mobility upon increasing the Brij 35 concentration. This behaviour, observed for three different methanol contents (40, 50 and 60%, v/v) may be explained concomitantly by an increase in the electrolyte viscosity and by the adsorption of the surfactant on the capillary wall. The build-up of Brij 35 on the surface of bare silica capillaries was also observed by Ahuja et al. [17] with a phosphate buffer, pH 7.0 and was blamed for irreproducible
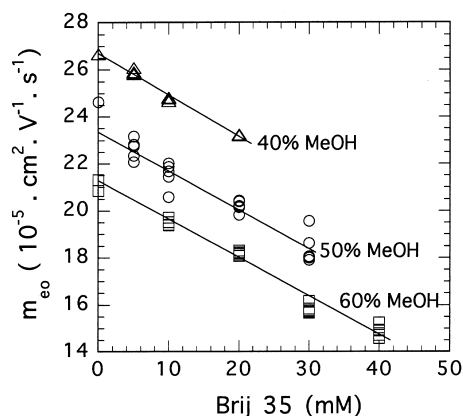
Fig. 8. Dependence of the electroosmotic mobility on Brij 35 concentration for various methanol contents in the electrolyte. Same conditions as in Fig. 7.

Fig. 9. MEKC separation of a standard mixture of linear saturated and unsaturated FFAs. Fused-silica capillary, 35 cm (27.5 cm to the detector cell)×50 μm I.D. Electrolyte, 10 mM Tris–5 mM p-anisate (pH 8.1) containing 10 mM Brij 35 (polyoxyethylene-23-lauryl ether) in methanol–water (50:50, v/v). Applied voltage, 30 kV (I=4 μA). Temperature, 25°C. Indirect absorbance detection at 254 nm. Gravity injection of the sample mixture (2· 10^{-4} M each in the electrolyte) for 5 s (injection volume, 2 nl). In $C_{n:m}$, the total number of carbon atoms, n, and the number of ethylenic bonds, m, are meant. Electroosmotic mobility, m_{eo}= $19.9 \cdot 10^{-5}$ cm^2 V^{-1} s^{-1}. Average peak efficiency, N=90 000.

migration times and corrected peak areas. As revealed by the points displayed in Fig. 8, rather scattered measurements were also obtained in this work from iterative experiments. Although the capillary had been flushed, before any measurement, with a volume of electrolyte corresponding to 6-times its inner volume, this scatter can be ascribed to incomplete equilibration.

Fig. 9 illustrates the optimized separation of a standard mixture of eight FFAs of practical interest. The carrier electrolyte consisted in 10 mM Tris–5 mM p-anisate (pH 8.1) with 10 mM of Brij 35 as buffer additive, in a methanol–water (50:50, v/v) mixture. Under the cathodic EOF (m_{eo}=$19.9 \cdot 10^{-5}$ cm^2 V^{-1} s^{-1}) that is created in such conditions, FFAs were detected in order of decreasing chain length, i.e., the C$_{20:0}$ acid (m_{eff}= $-2.1 \cdot 10^{-5}$ cm^2 V^{-1} s^{-1}) and the C$_{14:1}$ acid (m_{eff}= $-8.1 \cdot 10^{-5}$ cm^2 V^{-1} s^{-1}) corresponding to the first and the last peak, respectively. This small mobility difference suggests that the baseline separation of complex mixtures of PUFAs will be difficult, because of the limited migration window that is expected in such system. In addition, when separating mixture of PUFAs by chromatographic techniques, it is well known that each double bond produces a decrease in retention time approximating that of two methylene groups. This is in agreement with the general concept of equivalent chain length (ECL). For PUFAs, ECL values can be calculated according to the following
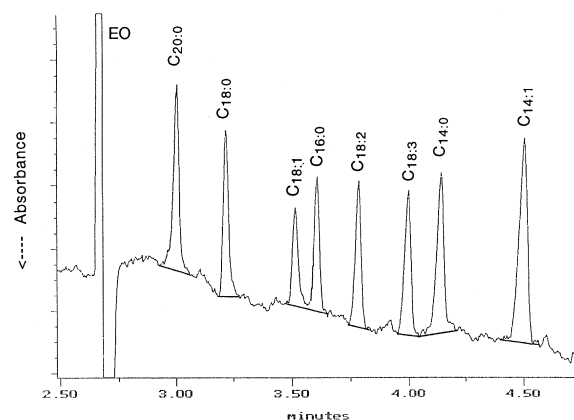
relationship: ECL=$N_c - 2N_{c=c}$, where N_c and $N_{c=c}$ correspond to the total number of carbon atoms and the number of double bonds, respectively. In the present case, the use of Brij 35 micelles allows the separation of compounds of common ECL (i.e., critical pairs), such as the pairs C$_{16:0}$/C$_{18:1}$ (ECL= 16), C$_{14:0}$/C$_{18:2}$ (ECL=14) and C$_{14:1}$/C$_{18:3}$ (ECL= 12).

4.2. Determination of a chromatographic-type selectivity

The determination of the selectivity afforded by Brij 35 micelles acting as a separating agent, i.e., of a selectivity of chromatographic-type defined according to Eq. (26), first requires the knowledge of the analyte affinity factors ($\tilde{k}'$). As discussed in Section 2, the calculation of the affinity factors in turn implies access to the effective mobilities of the analytes in the absence of the neutral surfactant. The FFAs having ECL in excess of 20, however, are not soluble without micelles in hydroorganic electrolytes solely containing 40 to 60% methanol. This ex-
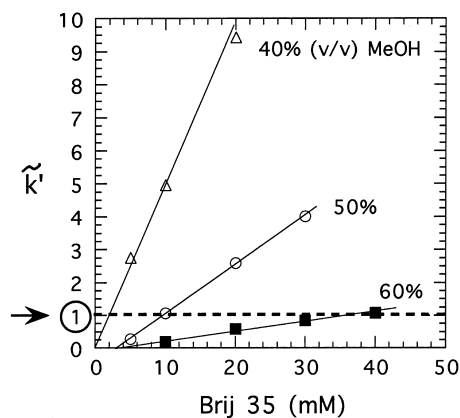
Fig. 10. Influence of Brij 35 concentration on the experimental values of the $C_{16:0}$ FFA affinity factor ($\tilde{k}'$) for various methanol contents in the electrolyte. $\tilde{k}'$ values were calculated from data shown in Fig. 7 using Eq. (22). The straight line $\tilde{k}' = 1$ is drawn in dashed line (see Section 4.2 for comments).

perimental limitation led us to concentrate on the $C_{16:0}/C_{18:0}$ pair. The calculation of the affinity factors also needs the electroosmotic mobility be determined. In the presence of neutral micelles, this issue does not bring about any additional experimental constraint: as the micelles move at the velocity of the EOF, any neutral marker, polar or apolar, can be selected for that purpose. It must be recalled that, in the classical case of MEKC (neutral analytes/anionic micelles), the determination of retention factors requires the measurements of t^* and t_{eo}, which goes

through the tricky choices of micellar and EOF markers.

Fig. 10 shows the variation of the affinity factor $\tilde{k}'$ as a function of the total concentration of Brij 35 in the electrolyte for the C_{16} linear saturated FFA. As expected from Eq. (2), straight lines were obtained. The slopes of these lines, which are to be proportional to the analyte distribution coefficient, decrease on increasing the methanol content. As far as resolution optimization is concerned, it is desirable that $\tilde{k}'$ should be smaller than 1. Purposely, the dashed line $\tilde{k}' = 1$ was also drawn to better evaluate optimal surfactant concentrations. It appears that with 40% methanol, $\tilde{k}'$ is already in excess of 1 for Brij 35 concentrations as low as 5 mM. With 50% methanol, $\tilde{k}'$ reaches the value of 1 for ca. 10 mM Brij 35, while for 60% methanol, $\tilde{k}'$ remains lower than 1 in almost the whole concentration range of practical interest. Similar conclusions can be drawn for the linear saturated $C_{18:0}$ FFA from inspection of Fig. 11. These results can be confronted with the variation of resolution of the $C_{16:0}/C_{18:0}$ pair, calculated directly from experiment, vs. surfactant concentration. In fact, in order to eliminate the influence of plate number, Fig. 12 displays the variation of $\tilde{R}_s$, which according to Eq. (11) is to be equal to:

$$\tilde{R}_s = \frac{4R_s}{\sqrt{\bar{N}}} = \left| \frac{m_1^{eff} - m_2^{eff}}{\bar{m}^{eff} + m_{eo}} \right| \tag{32}$$
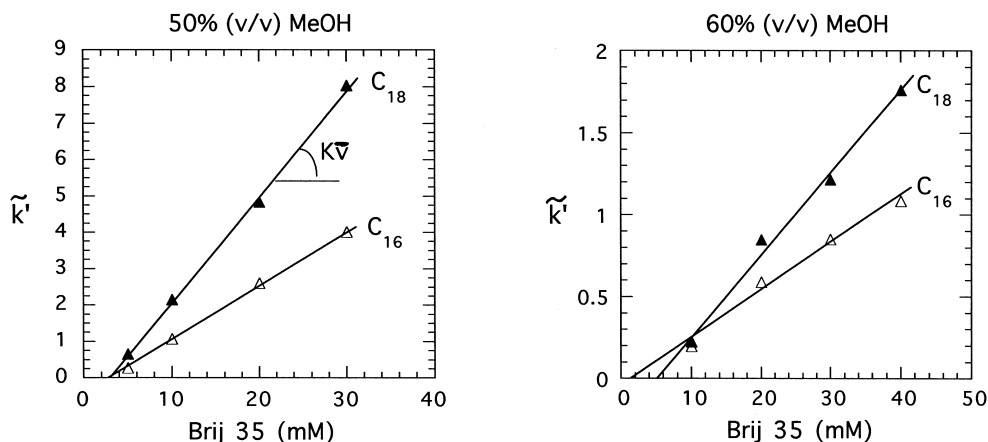
According to Fig. 12, the resolution is poor with

Fig. 11. Influence of Brij 35 concentration on the experimental values of the affinity factor ($\tilde{k}'$) of the $C_{16:0}/C_{18:0}$ pair for (a) 50% and (b) 60% (v/v) methanol in the electrolyte. $\tilde{k}'$ values were calculated from data shown in Fig. 7 using Eq. (22).
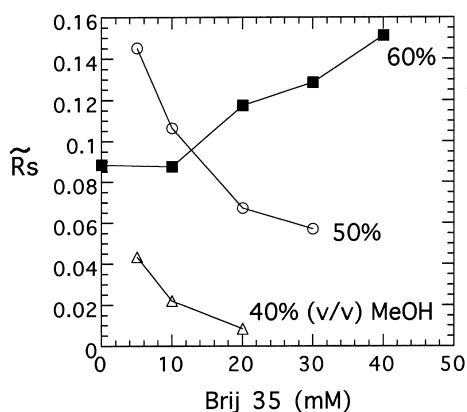
Fig. 12. Experimental dependence of the $C_{16:0}/C_{18:0}$ $\tilde{R}_s$ values on Brij 35 concentration for various methanol contents in the electrolyte. $\tilde{R}s$ values were calculated from data shown in Figs. 7 and 8 using Eq. (32). See Section 4.2 for explanations.

40% methanol, which is in keeping with too high values of $\tilde{k}'$. The higher the Brij 35 concentration is, the lower $\tilde{R}_s$ is because $\tilde{k}'$ values are getting farther from optimal values. With 50% methanol, $\tilde{R}_s$ takes the highest value for 5 mM Brij 35 (the $\tilde{k}'$ values are lower than 1, see Fig. 11) but is seriously impaired when Brij 35 concentration is increased. The tendency is reversed with 60% methanol, $\tilde{R}_s$ becomes an increasing function of Brij 35 concentration in the range 10–40 mM, because the $\tilde{k}'$ values are inferior to 1 (Fig. 11) and are getting closer to optimal values. The linear regressions on data reported in

Fig. 11 also give access to the separation selectivity of the $C_{16:0}/C_{18:0}$ pair, applying Eqs. (2) and (26). The results are given in Table 1 and compared to literature data derived from gas (GC) and liquid (LC) chromatography experiments. It can be concluded that the use of Brij 35 micelles in MEKC brings about quite similar selectivity values (around 1.8) as those afforded by GC with either apolar or polar phases. Lower selectivity values were calculated, however, from the two literature data derived from reversed-phase LC (1.25 to 1.4). The fact that these data were derived from gradient elution experiments should account for these lower values. Rigorously no selectivity calculation can be done from gradient elution. Nevertheless in practice, the low slope of the gradient made it possible to consider this result as an approximate selectivity value. This lower selectivity in LC is compensated by an infinite retention range and high retention factors (ca. 10 for $C_{16:0}$ and $C_{18:0}$ FFAs in Ref. [20]), so that the retention term of Purnell equation reaches about 0.9 in LC $[k'/(1+k')\sim0.9]$ whereas f($\tilde{k}'_{opt}$) is kept below 0.3 for the present case in MEKC, considering that the t^0/t_{eo} ratio ranges from 1.5 to 3.5.

Finally, the determination of the x-intercept of the straight lines in Fig. 11 should provide an estimation of the CMC values of Brij 35 in the media studied. With 50% methanol, the straight lines pertaining to the $C_{16:0}$ and $C_{18:0}$ FFAs converged on the x-axis toward the value 2.94 mM and 2.85 mM, respective-

Table 1
Calculated values of selectivity (α) for the $C_{16:0}/C_{18:0}$ pair from this work (see Fig. 11) and literature data

Source	Method	Micellar pseudo-phase or stationary phase	Electrolyte or mobile phase	α
This work (Fig. 11)	MEKC	Brij 35 micelles	MeOH–water 60:40, v/v 50:50, v/v	1.70 1.96
Ref. [18]	GC	SPB-1 (hydrophobic)	Helium	1.85
Ref. [18]	GC	SP-2380 (polar)	Helium	1.75
Ref. [19]	LC	Alkyl C_8 coated silica 5 μm	MeOH–water (85:15 to 100:0, v/v)	1.25
Ref. [20]	LC	Spherisorb ODS-2 5 μm	ACN–water (79:21 to 99:1, v/v)	1.40

GC = gas chromatography (isothermal); LC = liquid chromatography (gradient elution); SPB-1 = poly(dimethylsiloxane); SP-2380 = poly(90%-biscyanopropyle–10%-cyanopropylphenylsiloxane).

ly. A value of 3.0 mM for the CMC can be retained in this medium. With 60% methanol, however, both straight lines failed to cross each other on the x-axis. This latter result does not call the validity of Eq. (2) into question. Rather, the presence of solely four experimental points on each curve should be considered.

5. Conclusions

The study of the separation of saturated and unsaturated FFAs has given us the opportunity to extend the physico-chemical model for MEKC initially developed by Terabe et al. [12] (neutral analytes/anionic micelles) to the case of anionic analytes in the presence of neutral micelles. The interest of this approach is double-facetted. It has allowed first to conduct the optimization of the resolution of a complex standard mixture as a function of the two main operating parameters (neutral surfactant concentration and organic solvent content) in a more rational and predictive way. In addition, it has been established that chromatographic-type selectivities can also be determined for analyte classes such as FFAs. The interest for defining selectivity likewise has been recently discussed and illustrated in the field of chiral separations by our group and others [16,21–23]. This allows mainly to parallel electrokinetic and conventional chromatographic techniques on a pure selectivity basis. It can be asserted from this work that the selectivity afforded by Brij 35 micelles, considered as a separating agent, with respect to FFA homologues is quite similar to that obtained with the usual GC phases.

More specifically, the potential of MEKC for the rapid resolution (<5 min) of several critical pairs of saturated and unsaturated FFAs of identical ECL has been demonstrated. In comparison to the conditions previously reported by Erim et al. [10], a chromophore agent (anisate) that do not take part in the formation of the micellar phase was used here. This resulted in both expanding the retention range and reducing the noise of the absorbance signal. Additionally, acetonitrile was replaced by methanol, which enhanced analyte solubility and decreased the

EOF and resulted in improved resolution for the $C_{14}-C_{20}$ FFAs.

Finally, the results presented in this paper provide further evidence that capillary electrophoretic techniques as a whole are well suited for the analysis of ionic surfactants, among which fatty acids are likely to be the most common ones. Apart from already recognized economical advantages such as the rapidity of the separations, the low cost of fused-silica capillaries, the negligible consumption in organic solvents and the lower demand in sample pretreatment, these techniques primarily offer a great flexibility for the adjustment of the separation selectivities, with a minimum time consumption in method development. While short and medium chain surfactant homologues can be very simply separated according to their mass difference in plain aqueous or hydroorganic electrolytes, long chain ($C_{10}-C_{20}$) homologues or complex mixtures of saturated, unsaturated, linear or branched surfactants are amenable to separate in the presence of various separating agents such as cyclodextrins or neutral micelles. The selectivity required for a typical application can be finely tuned by varying the nature, the concentration and the composition of the additives to the electrolyte. Nevertheless, the current detection limits imposed by indirect absorbance do not meet the requirements for trace analysis in biological or environmental samples. In this prospect, chemical derivatization strategies for the introduction of fluorogenic moieties that would be consistent with electrophoretic techniques remain to be explored.

References

[1] J. Romano, P. Jandik, W.R. Jones, P.E. Jackson, J. Chromatogr. 546 (1991) 411.

[2] C.S. Weiss, J.S. Hazlett, M.H. Datta, M.H. Danzer, J. Chromatogr. 608 (1992) 325.

[3] P.L. Desbène, C. Rony, B. Desmazières, J.C. Jacquier, J. Chromatogr. 608 (1992) 375.

[4] S. Chen, D.J. Pietrzyk, Anal. Chem. 65 (1993) 2770.

[5] G. Gutnikov, W. Beck, H. Engelhardt, J. Microcol. Sep. 6 (1994) 565.

[6] S.A. Shamsi, N.D. Danielson, Anal. Chem. 67 (1995) 4210.

[7] C.-E. Lin, W.-C. Chiou, W.-C. Lin, J. Chromatogr. A 722 (1996) 345.

[8] R. Roldan-Assad, P. Gareil, J. Chromatogr. A 708 (1995) 339.

[9] J. Collet, P. Gareil, J. Cap. Electrophor. 3 (1996) 77.

[10] F.B. Erim, X. Xu, J.C. Kraak, J. Chromatogr. A 694 (1995) 471.

[11] S. Terabe, K. Otsuka, K. Ichikawa, T. Ando, Anal. Chem. 56 (1984) 111.

[12] S. Terabe, K. Otsuka, T. Ando, Anal. Chem. 57 (1985) 834.

[13] M.T. Ackermans, F.M. Everaerts, J.L. Beckers, J. Chromatogr. 585 (1991) 123.

[14] J.P. Foley, Anal. Chem. 62 (1990) 1302.

[15] P. Gareil, Chromatographia 30 (1990) 195.

[16] F. Lelièvre, A. Jardy, P. Gareil, Anal. Chem. 69 (1997) 385.

[17] E.S. Ahuja, E.L. Little, K.R. Nielsen, J.P. Foley, Anal. Chem. 67 (1995) 26.

[18] G. Gutnikov, J. Chromatogr. B 671 (1995) 71.

[19] T. Ohshima, K.-I. Miyamoto, R. Sakai, J. Liq. Chromatogr. 16 (1993) 3217.

[20] J.F. Lawrence, C.F. Charbonneau, J. Chromatogr. 445 (1988) 189.

[21] S.G. Penn, E.T. Bergström, D.M. Goodall, J.S. Loran, Anal. Chem. 66 (1994) 2866.

[22] S. Piperaki, S.G. Penn, D.M. Goodall, J. Chromatogr. A 700 (1995) 59.

[23] D.K. Lloyd, A. Ahmed and F. Pastore, Electrophoresis, submitted for publication.